JOURNAL OF GEOPHYSICAL RESEARCH, VOL. 103, NO. B10, PAGES 23,827–23,838, OCTOBER 10, 1998

Earthquakes, volcanoes, and rectified diffusion

E. E. Brodsky

Seismological Laboratory, California Institute of Technology, Pasadena

B. Sturtevant

Graduate Aeronautics Laboratories, California Institute of Technology, Pasadena

H. Kanamori

Seismological Laboratory, California Institute of Technology, Pasadena

Abstract. Rectified diffusion is a mechanism by which a strain wave can rapidly pump volatiles into a bubble and therefore increase the pressure in a closed system. The dynamic strain of either distant regional tectonic earthquakes or local volcanic tremor can be translated to static strain inside a magma chamber via this process. We formulate a theory appropriate to the conditions of a magma chamber and calculate the increased pressure using realistic physical parameters. For a basaltic system initially at 130 MPa pressure, the excess pressure from rectified diffusion is between 0.4 and 4 MPa for a regional $M \geq 8$ earthquake. The pressure from rectified diffusion is often significantly above the static stress caused by deformation for documented cases of triggered eruptions and thus presents a more viable mechanism for triggering. Prolonged tremor can have a similar effect since the total pressure added increases linearly with the duration of the excitation.

1. Introduction

Earthquakes are often used empirically to forecast volcanic eruptions. However, the precise relationship between seismicity and magmatic activity remains enigmatic. In some cases, e.g., swarms, earthquakes are taken to be indicative of magma movement and therefore symptomatic of volcanic unrest. In other cases the relationship is apparently causal. There are a few documented cases of distant regional earthquakes triggering eruptions. In 1835, Darwin observed four volcanoes erupting after a large earthquake (M=8.5) on the Chilean coast [*Darwin,* 1896]. *Newhall and Dzurisin* [1988] document 50 cases of large regional earthquakes followed by caldera unrest. The only historical eruptions of both the Tao-Rusyr caldera and the Karpinsky group volcanoes occurred within days of a M=8.3 earthquake [*Kimura,* 1978]. In this study we limit ourselves to 11 of the best documented eruptions immediately following distant regional earthquakes. The eruptions we consider, shown in Figure 1, were triggered by large tectonic events over 100 km away. Previous work has attempted to explain triggered eruptions by computing the static stress change from elastic deformation [*Yamashina and Nakamura,* 1978; *Barrientos,* 1994]. The stress change thus computed can be as low as 100 Pa in some cases. These stresses are comparable to tidal stresses and therefore it is difficult to justify triggering a volcanic eruption. We present an alternative mechanism to relate large, distant regional earthquakes to eruptions.

A candidate mechanism would likely use the dynamic strain from distant regional earthquakes, of the order of 10^{-5}, to trigger activity. One such mechanism is rectified diffusion of dissolved vapor into preexisting bubbles in a magma body. Such bubbles exist in many natural systems as documented from melt inclusions [*Lowenstern,* 1995], volatile contents that exceed saturation at moderate depths [*Johnson et al.,* 1994], and evidence of coexisting gas phases in magma chambers [*Lambert et al.,* 1985]. When subjected to seismic waves, these bubbles expand and contract. Assuming the bubbles are originally near equilibrium with the vapor dissolved in the melt, when the bubbles contract, the vapor is oversaturated inside the bubble and diffuses out to the melt (See Figure 2). When the bubbles expand, the vapor is undersaturated inside and diffuses in from the melt. Since the surface area of the expanded bubble is larger than the contracted one, the mass transfer process is not symmetric. There is a net flow of vapor into the bubble, and if bubble growth is limited by the total compressibility of the system, a pressure increase results. In addition, the diffusive layer is thicker during the contracting phase, resulting in a reduced concen-

Paper number 98JB02130.
0148-0227/98/98JB-02130$09.00

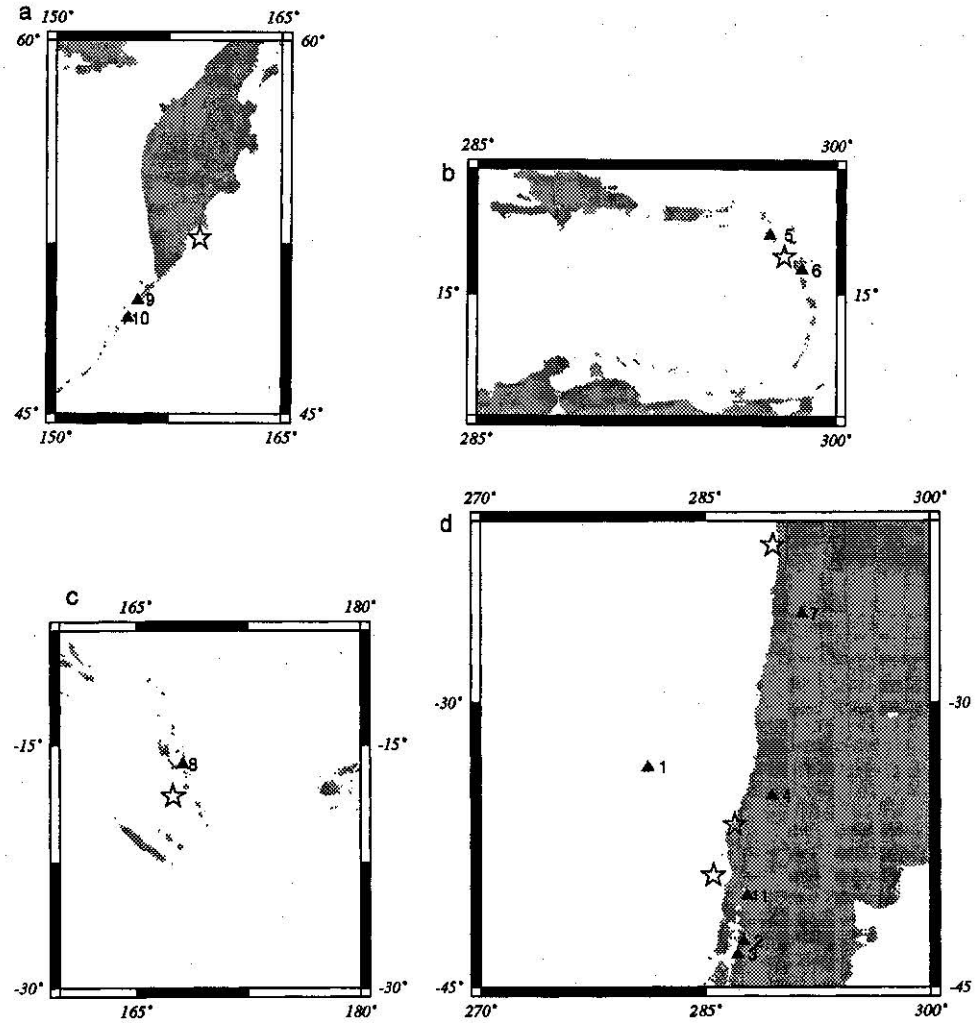

Figure 1. Location of volcanoes and earthquakes studied in this paper. The regions mapped are (a) Kamchatka, (b) the Caribbean, (c) the Southwest Pacific and (d) Chile. Triangles represent volcanoes and stars represent earthquakes. The numbers correspond to the following eruptions detailed in Table 2: 1, 1835 Robinson Crusoe; 2, 1835 Minchinmavida; 3, 1835 Cerro Yanteles; 4, 1835 Peteroa; 5, 1843 Liamuiga;, 6, 1843 unnamed; 7, 1877 Llullaillaco; 8, 1950 Ambrym; 9, 1952 Karpinsky group; 10, 1952 Tao-Rusyr caldera; 11, 1960 Puyahe.

tration gradient and slower mass transport than that during the expanded phase. This "shell effect" [*Eller and Flynn*, 1965] results in a further net mass flux into the bubble. Since the pressures in the bubble and the magma are the same except for a small surface tension term, an increase in the pressure inside a bubble translates to an increase in pressure in the entire fluid system. Bubble growth via rectified diffusion in constant pressure systems has been demonstrated by a number of experiments [e.g.,*Eller* [1969] and it is used in industrial applications such as ultrasonic cleaning. However, the increase in pressure in systems where expansion is restricted is a new feature of the formulations of *Sturtevant et al.* [1996] and this paper. Once the pressure increase occurs, a variety of mechanisms, including failure of the chamber, may ultimately result in an eruption.

The limitations and assumptions of rectified diffusion as a pressure-increasing mechanism in natural magmatic systems are explored in sections 2-8. We present a model of rectified diffusion in magmatic systems which is closely related to the theory of *Sturtevant et al.* [1996] for geothermal systems in sections 2-3. We then specify the necessary constraints on the system and numerically estimate the magnitude of the effect in sections 4-7. The computed stresses are compared to static stress changes in an elastic halfspace in section 7 and we discuss the implications for documented triggering cases.

2. Model Overview

We derive an expression for the increase of pressure produced by a seismic wave passing through a bubbly magma chamber by beginning with an equation of state for the volatiles in the bubble. The strategy of this paper is to use this equation of state to write an equation for the evolution of pressure in the bubble (and hence

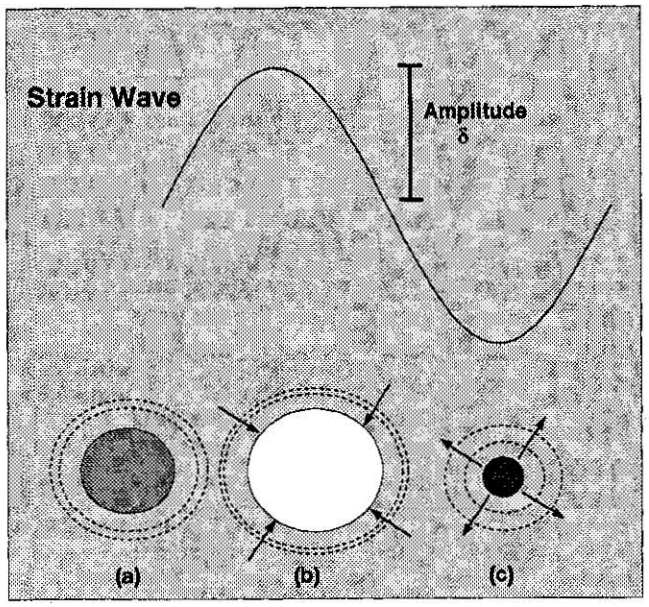

Figure 2. Cartoon of rectified diffusion. As the system is excited by a seismic wave, a bubble that is (a) initially in equilibrium is (b) expanded and then (c) compressed. The shading inside the bubble represents the volatile concentration. During the expansion phase (Figure 2b) the concentration is lower inside the bubble, and hence volatiles diffuse into the bubble as shown by the arrows. During the compression phase (Figure 2c) volatiles diffuse out of the bubble that has a higher concentration inside. The dashed outer circles represent a shell of constant volume. During expansion the shell is thinner, thus resulting in a faster diffusive flux than when the shell thickens during compression [*Leighton*, 1994]. The diffusive layer surrounding the bubble should be less than the radius of the bubble in order to be in strict accordance with the formulation of *Hsieh and Plesset* [1961]. In this paper the depleted layer is approximately the same size as the bubble, but this has only a minor effect.

the system) in terms of the evolution of the volume of the bubble and the mass inside the bubble. The mass inside the bubble can then be constrained by the rectified diffusion mass flux of *Hsieh and Plesset* [1961], and the volume of the bubble can be determined by considering the balance in volume changes over the entire magma-volatile system. The result is a rate of pressure increase as a function of the physical parameters of the system.

3. Theory of Rectified Diffusion in Magmatic Systems

For the high pressures and temperatures of a magmatic system, the modified Redlich-Kwong(MRK) equation of state is appropriate for the volatiles [*Holloway*, 1977],

$$P = \frac{RT}{v-b} - \frac{a}{(v^2+bv)T^{1/2}} = \frac{RT}{V/n-b} - \frac{a}{[(V/n)^2+bV/n]T^{1/2}}, \quad (1)$$

where P is pressure, T is temperature, V is volume of a bubble, n is number of moles, R is the ideal gas constant, v is the molar volume ($= V/n$), a is an empirical function of temperature, and b is an empirical constant. We differentiate (1) with respect to time and arrive at an expression for the rate of pressure change $\dot{P}$ in terms of $\dot{V}$ and $\dot{n}$,

$$\dot{P} = \frac{n\dot{V} - \dot{n}V}{n^2}\left[\frac{-RT}{(v-b)^2} + \frac{a(2v+b)}{(v^2+bv)^2T^{1/2}}\right]. \quad (2)$$

We must evaluate $\dot{n}$ and $\dot{V}$ in order to derive $\dot{P}$ as a function of the state of the system.

We hypothesize that the method for increasing the mass inside the bubbles is rectified diffusion. Note that $\dot{n} = \dot{m}/M_v$ where M_v is the molecular weight of the volatile and $\dot{m}$ is the rate of mass addition by rectified diffusion. *Hsieh and Plesset* [1961] combine the contributions of each half cycle of an oscillating bubble (Figure 2) to derive the mass flux of rectified diffusion as

$$\dot{m} = 24\pi DC_s r_0 \delta^2, \quad (3)$$

where D is the diffusivity, C_s is the saturated volatile concentration at the mean ambient pressure in the magma far from the bubble, δ is the amplitude of the dynamic strain wave, and r_0 is the bubble radius. In the natural system, δ is the amplitude of the seismic waves in the magmatic body since most of the compression of the magma-volatile solution occurs in the bubbles.

In order to evaluate the rate of volume change of an individual bubble, $\dot{V}$, one must look at the conservation of volume of the whole system, V_S,

$$\dot{V}_S = \dot{V}_M + N\dot{V}. \quad (4)$$

V_M is the volume of the magma, and N is the number of bubbles in the system. $\dot{V}_S$ can be nonzero owing to two distinct processes: (1) leakage of fluid (magma or volatiles) out of the system and (2) deformation of the magma chamber walls. The importance of the first process can be calculated by assuming that fluid percolates out of the chamber following Darcy's law of flow through porous media. The ratio of elapsed time since the exciting earthquake divided by a characteristic time for percolation provides a measure of the importance of such leakage. This nondimensional number is

$$4P(k/\mu)t/L^2, \quad (5)$$

where k is permeability, μ is viscosity, L is a characteristic length of the magma body and t is time. Typical values of k are of the order of a millidarcy (10^{-15} m^2), and L is assumed to be at least 100 m. If the leaking fluid is magma, the ratio is never above 10^{-6} for the results presented here. Even the leakage of steam, which has a much lower viscosity, would not affect the pressure until after ~100 days. During the earthquake, percolation is negligible and is not relevant to the mass balance in (4).

The second process, deformation of the walls, can be evaluated by assuming that the chamber walls are compressed elastically by the increasing pressure in the system. Simplifying the geometry to a sphere,

$$\frac{U_{rr}}{L} = \frac{P}{4G}. \tag{6}$$

U_{rr} is the radial displacement, L is the radius of the magma chamber, and G is the shear modulus of the country rock [*McTigue,* 1987]. Therefore the elastic contribution to the change in V_S is

$$\dot{V}_S = \frac{\pi L^3}{G}\dot{P}. \tag{7}$$

With increasing pressure, the magma will also compress elastically, and the magma volume change will be

$$\dot{V}_M = \beta V_M \dot{P}, \tag{8}$$

where β is the isothermal compressibility of the magma $1/V\,(\partial V/\partial P)_T$.

Combining (2),(4), (7) and (8),

$$\dot{P}\left(1 - \frac{V_S[\frac{3}{4}\frac{1}{G} - \beta(1-\phi)]}{Nn}A\right) = \frac{-V\dot{n}}{n^2}A, \tag{9}$$

where

$$A = \frac{-RT}{(v-b)^2} + \frac{a(2v+b)}{(v^2+bv)^2T^{1/2}} \tag{10}$$

and the porosity ϕ is defined by

$$\phi = \frac{NV}{V_S}. \tag{11}$$

If the term

$$-\frac{V_S[\frac{3}{4}\frac{1}{G} - \beta(1-\phi)]}{Nn}A \tag{12}$$

is much less than 1, the volume change of the bubbles will be negligible. This criterion can be rewritten in terms of porosity ϕ as

$$\phi \gg \phi_{th} \equiv \frac{vA(\frac{3}{4}\frac{1}{G} - \beta)}{1 - vA\beta}, \tag{13}$$

where ϕ_{th} is the threshold porosity. Equation (13) explains why a single small bubble does not increase the pressure in a chamber. If there are too few bubbles, the compressibility of the magma and the surrounding rock allows the bubbles to change in size and the resulting pressure change is small. The exact values of the parameters in Equation (13) depend on the chemistry of the volatiles and the ambient pressure. The elastic moduli $-\beta$ and $1/G$ are $\sim 10^{-10}$ Pa^{-1}. Typical values for the molar volume v and the constant A are 0.1 m^3 mol^{-1} and -2×10^2 MPa, respectively. For water bubbles at 1.3×10^2 MPa pressure (lithostatic pressure at a depth of 5 km), ϕ_{th} is 0.026. For CO_2 at the same conditions, ϕ_{th} is 0.037. Temperature and composition dependence in both cases is fairly weak. Since we have already assumed the existence of bubbles, exceeding these small thresholds is not a difficult additional constraint. For the remainder of this work we will assume that the porosity ϕ exceeds the threshold porosity ϕ_{th}.

If the porosity of the system satisfies (13) then (9) simplifies to

$$\dot{P} = \frac{-\dot{n}}{n}v\left[\frac{-RT}{(v-b)^2} + \frac{a(2v+b)}{(v^2+bv)^2T^{1/2}}\right]. \tag{14}$$

We linearize (14) by assuming that departures from the initial state are small, $v = v_0$ and $n = n_0$. Assuming a spherical bubble, the initial number of moles n_0 is given by

$$n_0 = \frac{4\pi r_0^3 \rho}{3M_v}, \tag{15}$$

where ρ is the initial density in the bubble.

Substituting (3) and (15) into (14),

$$\dot{P} = \frac{-18DC_s\delta^2}{r_0^2\rho}v_0\left[\frac{-RT}{(v_0-b)^2} + \frac{a(2v_0+b)}{(v_0^2+bv_0)^2T^{1/2}}\right]. \tag{16}$$

$\dot{P}$ can be easily calculated from (16) for any P, T condition. Note that if a and b were zero, the equation of state would reduce to the ideal gas law, and (16) would become equation (15) of *Sturtevant et al.* [1996]. The right-hand side of (16) is constant, and therefore the final pressure attained depends linearly on the duration of ground motion. The appropriate values of a and b are provided by *Holloway* [1977]. The diffusivity D and the concentration C_s can be estimated from laboratory data as a function of pressure and temperature for a given magma-volatile chemistry (see Table 1). The final pressure depends on the squares of the bubble radius r_0 and dynamic strain δ. Both parameters must be constrained by observations of natural systems.

4. Volatile Concentration

Hsieh and Plesset [1961] derived equation (3) for the mass flux assuming that the solution was saturated. For solutions that are supersaturated or subsaturated the flux due to ordinary diffusion must be superposed on the rectified diffusion flux. In a bubbly system with restricted volume changes, the pressure will rise as long as the total mass flux is positive into the bubble even if the ordinary diffusive mass flux is outward, i.e., the solution is subsaturated. The threshold for a pressure rise can be derived by setting the mass flux due to ordinary diffusion equal to the rectified diffusion mass flux. The ordinary diffusive mass flux is approximately [*Strasberg,* 1961]

$$4\pi D r_o\left[C_\infty - C_s(1 + \frac{2\sigma}{r_0 P_0})\right], \tag{17}$$

where C_∞ is the volatile concentration in the fluid far from the bubble, P_0 is the ambient pressure, and σ is

Table 1. Calibration Data for Solubility and Diffusivity Calculations

Variables	References	Pressure Range, GPa	Temperature Range, °C
Value a and b for CO_2 in MRK	*Holloway* [1977]	0.1-1	100-1000
Value a and b for H_2O in MRK	*Holloway* [1977]	0.01-1 ; 0-0.1	20-1000 ; 0-1300
Solubility CO_2 in basalt	*Dixon* [1992] and *Pan et al.* [1991]	< 0.1 ; 1.0, 1.5	1200 ; 1300-1600
Solubility H_2O in basalt	*Dixon* [1995]	0.018-0.8	1100-1200
Solubility H_2O in rhyolite	*Silver et al.* [1990]	< 0.15	850
Diffusivity CO_2 in basalt	*Blank* [1993]	0.05-0.105[a]	350-1050[b]
Diffusivity H_2O in basalt	*Zhang and Stolper* [1991]	1.0[a]	1300-1500
Diffusivity H_2O in rhyolite	*Zhang et al.* [1991]	0.0001[a]	400-850

[a]No pressure dependence is modeled for diffusivity.
[b]These experiments were for granitic composition but pass close to the one basalt point of *Zhang and Stolper* [1991] as noted by *Watson* [1994].

the surface tension. Therefore the total mass flux into the bubble from both ordinary and rectified diffusion is

$$4\pi D r_o \left[C_\infty - C_s(1+\frac{2\sigma}{r_0 P_0})\right] + 24\pi D C_s r_0 \delta^2 \quad (18)$$

and this expression must be positive for the pressure to grow. Rewriting this statement as a threshold in terms of concentration produces

$$\frac{C_\infty}{C_s} > \left(1+\frac{2\sigma}{r_0 P_0}\right) - 6\delta^2. \quad (19)$$

Since δ for the dynamic strains considered here is $\sim 10^{-5}$, the last term is negligible and the fluid must be supersaturated in volatiles. Moreover, as the pressure rises, the solubility of the volatiles also rises; that is, C_s rises over time (see Figure 3.) The relative saturation C_∞/C_s decreases, and if it drops below the threshold in (19), the ordinary diffusive flux out of the bubble will be greater than the rectified diffusion flux into the bubble. The pressure increase will stop. For CO_2-magma systems it is appropriate to assume that C_s is linearly proportional to pressure P. We define the initial supersaturation x by

$$C_\infty = (1+x)C_s^0. \quad (20)$$

Since the initial saturation concentration C_s^0 is proportional to the initial pressure P_0 and the final C_s is proportional to the final pressure $\Delta P + P_0$, the left-hand side of (19) can be written as

$$\frac{C_\infty}{C_s} = \frac{(1+x)P_0}{P_0 + \Delta P}. \quad (21)$$

The maximum possible pressure rise ΔP is therefore governed by (19):

$$\Delta P < P_0 \left(-1 + \frac{1+x}{-6\delta^2 + (1+\frac{2\sigma}{r_0 P_0})}\right). \quad (22)$$

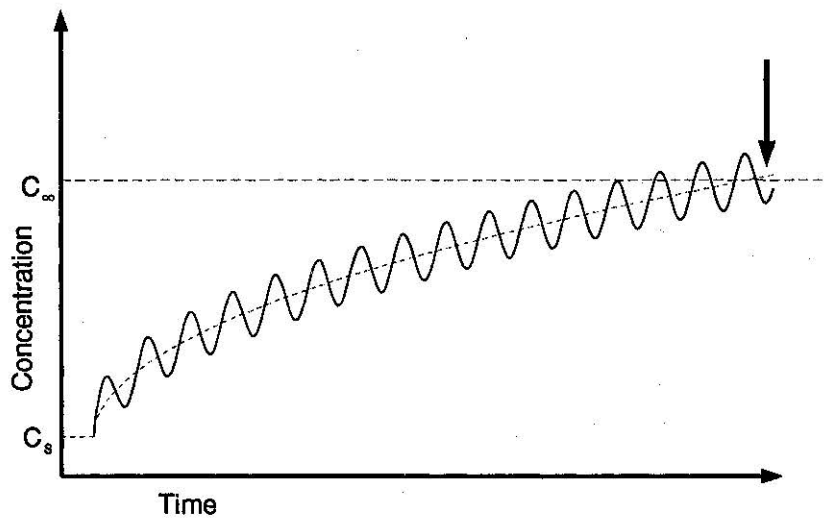

Figure 3. Schematic of the change in solubility with pressure. The solid sinusoid represents the concentration at the bubble wall. The dashed horizontal line indicates the far-field concentration C_∞, and the dotted curve is the saturation concentration C_s, which increases as the pressure increases. When C_s becomes greater than C_∞ by $\sim 6\delta^2$ at the time indicated by the arrow, the solution becomes subsaturated and rectified diffusion ceases.

If the system is supersaturated so that

$$1 \gg x \gg \frac{2\sigma}{r_0 P_0} - 6\delta^2, \tag{23}$$

then (22) can be approximated by

$$\Delta P < x P_0. \tag{24}$$

Equation (24 is appropriate for CO_2 in magmatic systems, but the concentration at saturation C_s of water in magmas at low pressures is not linear in pressure. For water dissolved in silicate melts C_s is better approximated as proportional to $P^{1/2}$ [*Silver et al*, 1990]. The maximum pressure increase for a given initial supersaturation is therefore slightly higher for water in magma and bounded by

$$\Delta P < P_0 \left[-1 + \left(\frac{1+x}{-6\delta^2 + (1 + \frac{2\sigma}{r_0 P_0})} \right)^2 \right]. \tag{25}$$

Using the same approximation as before, (25) to first order in x is

$$\Delta P < 2 x P_0. \tag{26}$$

ΔP is limited in both cases by the initial supersaturation. A 1% supersaturated solution can support approximately a 1% increase in pressure in a CO_2 system or a 2% increase in an H_2O system.

Given the necessity of supersaturation and hence a positive mass flux into the bubble before excitation, one might ask what effect the small increase in mass flux from rectified diffusion would have? Would not the pressure already be rising from diffusive growth in the supersaturated solution? Since the rectified diffusion mass flux is much smaller than the ordinary mass flux, why is it not negligible? To answer these questions, we postulate a quasi-steady state prior to the exciting earthquake. The magmatic system slowly became supersaturated during cooling and crystallization of the melt. On the same, slow timescale, volatile escape occurs as bubbles leave the supersaturated area or as gas percolates away. When an earthquake occurs, a small, uncompensated increase in mass flux occurs. Even though the rectified diffusion mass flux increase is much smaller than the total mass flux into the bubbles, the rapid excitation prevents the development of a compensating loss of volatiles. The pressure rises.

We have not modeled the initial supersaturated system in detail, but we can propose a scenario in which the necessary conditions would exist. In a highly heterogeneous magma body undergoing vigorous convection as first suggested by *Shaw* [1965], there will be some regions that are crystallizing and others that are resorbing mineral phases into the melt at any given time. As the system nears eruption, crystallizing regions that are undergoing second boiling and bubble growth should be common. During the preparatory stages of an eruption there may always be some region of the magma body that has recently become supersaturated and thus has small bubbles present. These regions would be the relevant areas for rectified diffusion to occur. This scenario highlights a few of the important requirements for triggering an eruption by dynamic strain. Rectified diffusion is a triggering mechanism. The magma-volatile system must already be present and exsolving gases. The volcanoes studied in this paper would have likely erupted eventually. The regional earthquakes merely accelerated the process. Also, the entire magma body need not be filled with small bubbles in order for rectified diffusion to occur. As long as a region has enough bubbles to meet the porosity constraint in (13) when normalized by the total volume of the magma body, then rectified diffusion will be an effective pressure-raising mechanism.

5. Physical Constraints

The rate of pressure increase is very sensitive to the bubble radius. In a multiple bubble system an effective radius for the entire system can be calculated. The total volume change of all the bubbles present is equal to the volume change of N bubbles of an effective radius r_{eff} [*Sturtevant et al.*, 1996]. In terms of average radius $\overline{r}$ and average cubed radius $\overline{r^3}$, the effective radius is

$$r_{\text{eff}} = \sqrt{\overline{r^3}/\overline{r}}. \tag{27}$$

Direct observation of the average bubble size in a magma chamber is impossible. It might be expected that one could learn about bubble sizes from natural volcanic samples. However, the rapid decompression during eruptions dominates the observed bubble size distribution, and no easily discernible information about the in situ magma chamber bubble sizes is retained in the rocks [*Cashman and Mangan*, 1994]. *Hurwitz and Navon* [1994] observed average bubble sizes as small as 5×10^{-6} m in laboratory nucleation experiments, and *Davis and Ihinger* [1996] observed 10^{-6} m bubbles in similar work. The critical radius for the most supersaturated solution considered in this study is 7×10^{-8} m. The critical radius places an extreme lower bound on the bubble radius and the experimental work gives an expected order of magnitude. We choose to model the effective bubble radius r_{eff} as 10^{-6} m. If future research shows another bubble size to be more appropriate, these results can be modified in accordance with (16). The total pressure accumulated during shaking is proportional to the inverse squared of the effective bubble radius.

The use of such small bubbles may raise the concern that surface tension effects are important. However, as shown by the formulation of *Crum and Hansen* [1982], surface tension only affects the mass flux if the Laplace pressure $2\sigma/r$ is of the same order as or greater than the ambient pressure P_0. For 10^{-6} m volatile bubbles in magmas, the Laplace pressure is of the order of 0.1

MPa, and P_0 is of the order of 100 MPa. Therefore surface tension is negligible.

The rate of pressure increase is also very sensitive to the amplitude of the dynamic strain wave, δ, at the location of the bubbles. Conventional estimates of the dynamic strain from regional earthquakes are for the measured hard-rock shear wave amplitudes δ_{hr} and therefore are not the relevant δ in the bubbly magma body. Calculating δ from δ_{hr} inevitably involves large uncertainties; we estimate that $\delta = 10\ \delta_{hr}$ by proposing the following scenario: (1) When shear waves enter a very heterogeneous magma chamber, mode conversion occurs and shear strain is converted to volumetric stain. This process results in some loss of energy but appears to be reasonably efficient since Love waves (transversely polarized shear waves) have been observed with water-well seismographs which are only sensitive to volumetric strain [*Carragan et al.*, 1964]. (2) As the waves enter a bubbly magma body, amplification occurs. The amplitude of the wave is increased due to conservation of energy. In addition, a complex series of reflections cause the structure to reverberate. The amplification can be roughly estimated by examining the model system of a soft layer between two half-spaces. The Fourier transform of the waveform $X(\omega)$ is the product of the incident spectrum $I(\omega)$ and the response function $G(\omega)$,

$$X(\omega) = G(\omega) \times I(\omega). \tag{28}$$

In a magma layer of width L between two hard-rock half-spaces, $G(\omega)$ for a point at a distance x into the magma chamber is

$$G(\omega) = \frac{V_{hr}}{V_{mag}} \frac{1+R}{1-R^2 e^{-2i\omega \frac{L}{V_{mag}}}} \cdot \left(e^{-i\omega \frac{x}{V_{mag}}} - Re^{-2i\omega \frac{L}{V_{mag}}} e^{i\omega \frac{x}{V_{mag}}} \right) \tag{29}$$

where R is the reflection coefficient

$$R = \frac{\rho_{hr} V_{hr} - \rho_{mag} V_{mag}}{\rho_{hr} V_{hr} + \rho_{mag} V_{mag}}. \tag{30}$$

ρ_{hr} and V_{hr} are the hard-rock density and P wave velocity; ρ_{mag} and V_{mag} are the magmatic density and P wave velocity. Laboratory experiments show that melts typically have densities ~5% less than their solid counterparts, and the P wave velocities of melts are ~50% less [*Murase and McBirney*, 1973]. A bubbly magma will have an even lower seismic velocity since the volatile phase is highly compressible [*Kieffer*, 1977]. A conservative estimate of the strain amplification is therefore provided by using the above laboratory values in (29). The strain entering a magma body ~1 km wide is amplified by at least a factor of 20. Since some energy of the wave is undoubtedly lost in mode conversion, a conservatively low value for the total amplification δ/δ_{hr} is 10. This estimate of the amplification factor is certainly approximate, and a range of 10-15 is studied in the model systems of this paper in order to demonstrate the sensitivity of the calculations.

An estimate of δ_{hr} for the historical events can be made by scaling observations of a well-documented earthquake. The hard-rock amplitude of seismic waves is assumed to be the same as that observed at well-placed seismometers. For the regional earthquakes discussed here we used the strong motion records of the 1985 M=8.1 Michoacan, Mexico earthquake and the scaling proposed by *Houston and Kanamori* [1990]. This earthquake provides a good analog for the large thrust events that commonly trigger arc volcanoes. The positions of the stations in Michoacan in relation to the fault rupture are similar to the positions of volcanoes along an arc. For very large earthquakes the amplitude of high-frequency waves depends primarily on distance, not magnitude. Since all the earthquakes considered in this work are of sufficient magnitude, it is reasonable to use the scaling

$$\delta_{hr} = \delta_M \left(\frac{r_M}{r} \right)^p, \tag{31}$$

where δ_{hr} and δ_M are the strain amplitudes in the earthquake of interest and the Michoacan earthquake, respectively. The distances from the hypocenter to the site being considered are r and r_M. The exponent p is a scaling factor which is 0.43 - 0.8 depending on frequency [*Houston and Kanamori*, 1990]. Note that the distance from the volcano to the rupture zone may be considerably less than the distance to the epicenter for large events since M= 8 earthquakes break over 100 km of fault. The scaling of *Houston and Kanamori* [1990] is designed to still be valid in these cases. We used r_M = 35 km and δ_M = 4.27 x 10^{-5}, which is the highest amplitude of any wave on this record. Since the pressure increase goes as δ^2, it is only necessary to account for the largest amplitude waves affecting the magmatic system. The dynamic strain δ_{hr} is typically of the order of 10^{-5} for the parameters considered here.

For large earthquakes the duration of the excitation, Δt, scales as the rupture duration $\mathcal{L}/\mathcal{V}$, where $\mathcal{L}$ is the fault length and $\mathcal{V}$ is the rupture velocity. $\mathcal{L}$ is ~1000 km for the M_w = 9.5 1960 Chilean earthquake. The largest amplitude waves are observed for about one half the rupture duration on the Michoacan records. Using the conventional seismic scaling relation $M_w \propto 2 \log \mathcal{L}$, we approximate the duration in seconds,

$$\Delta t = \frac{1}{2} \left(10^{\frac{M_w - 9.5}{2}} \frac{1000}{2.9} \right)., \tag{32}$$

where the rupture velocity is assumed to be 2.9 km s^{-1}.

6. Model Systems

Equation (16) was evaluated for model systems defined by a volatile (carbon dioxide or water) in an end-member magma (basalt or rhyolite.) The effects of tem-

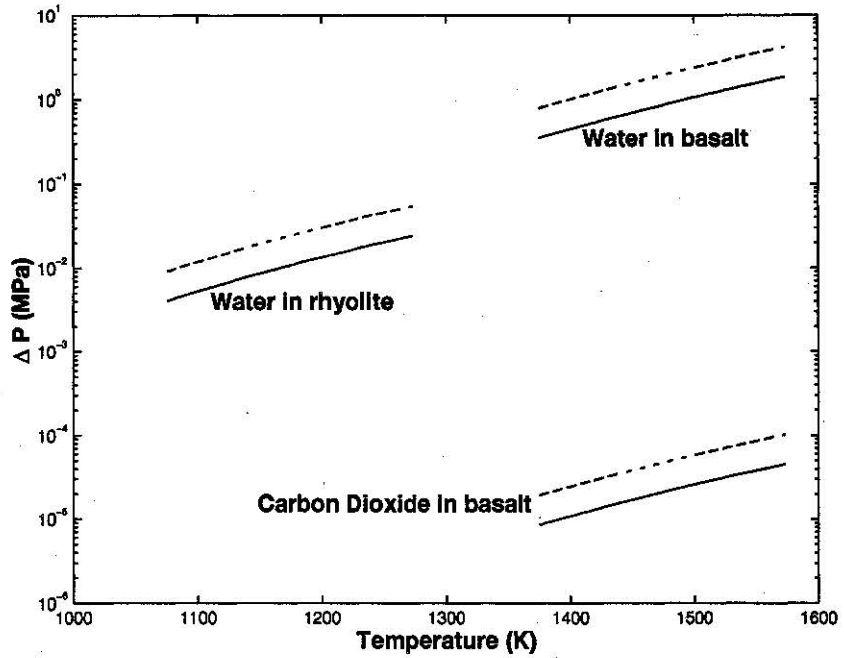

Figure 4. Temperature dependence of pressure increase ΔP in model systems via rectified diffusion. The dynamic strain measures 10^{-5} at the surface and lasts 30 s. The magma chamber is at 1.3 x 10^2 MPa (lithostatic pressure at 5 km depth). For each model system, two curves are plotted to show a range of amplification factors (δ/δ_{hr}) of 10-15.

perature and pressure are incorporated into the solubility and diffusivity estimates from laboratory data (see Table 1.) A range of values are considered, and the sensitivity of the results is shown in Figure 4 and Figure 5.

The temperature dependence of the pressure increase from rectified diffusion is shown in Figure 4; pressure dependence is shown in Figure 5. Figures 4 and 5 demonstrate the relative efficacy of different magma-volatile systems. Since the diffusivity of volatiles in basalt is much higher than that in rhyolite at natural temperatures, rectified diffusion is more effective in basaltic systems. For a basaltic system with water bubbles ini-

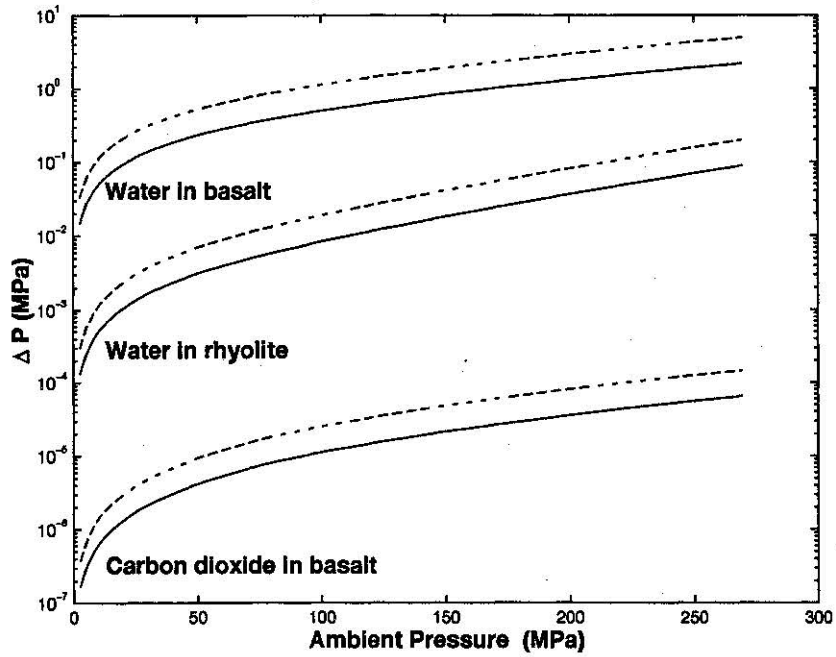

Figure 5. Pressure dependence of pressure increase ΔP in model systems via rectified diffusion. The basalt is modeled at 1450 K and the rhyolite is modeled at 1200 K. The excitation and ranges of amplification are the same as those in Figure 4.

tially at 130 MPa pressure, the excess pressure from rectified diffusion is between 0.4 and 4 MPa. Figures 4 and 5 show that when CO_2 is the dominant volatile in basaltic systems, the effect of rectified diffusion is very small. This difference arises because CO_2 is much less soluble in magmas than H_2O; that is, C_s is lower. Since the diffusivity of CO_2 in rhyolite is even lower than that of CO_2 in basalt [*Watson*, 1994] and the solubility is ~30% lower in rhyolite [*Blank*, 1993], the pressure increase will be even smaller than in the CO_2-basalt system. Therefore the CO_2-rhyolite system is not considered further in this work.

7. Historical Cases

Once a pressure increase occurs, a number of processes can eventually lead to dike propagation and a volcanic eruption. The nature of these mechanisms is uncertain and therefore the appropriate threshold for triggering an eruption is currently unknown. The goal of the present work is to show that rectified diffusion creates a much larger stress increase than the next most viable triggering mechanism. After the magma body is pressurized, the eruption can occur at any time. Since the magma-volatile solution is saturated or supersaturated at the end of the rectified diffusion process, the system can retain its pressure indefinitely. The pressure will be released either when an eruption occurs or when some other process such as percolation of gases continues for sufficient time (see equation (5)).

A number of instances of large tectonic events triggering volcanic eruptions have been documented. Demonstrating triggering is at best a subjective process. Occasionally, there is a particularly spectacular example such as the 1835 $M = 8.5$ Chile earthquake. Immediately after the earthquake, four eruptions began simultaneously. More often, the relationship is less clear. For this study, only eruptions occurring within 10 days of a large regional earthquake greater than 100 km from the volcano are considered. Table 2 lists some of the best-documented cases, and Table 3 shows the relevant modeling parameters. Locations are mapped in Figure 1.

Most of the earthquake-volcano systems can be approximated by one of the model cases shown in Figures 4 and 5. Where such an approximation was not possible, such as for the andesitic systems where no laboratory data are available, no further calculation was attempted. The calculated increase in pressure for all cases is less than 7%. Therefore the systems require at most 4% supersaturation in the bubbly region of the magma body in order to maintain rectified diffusion throughout the duration of shaking Δt in accordance with (25).

A crude estimate of the static stress is computed for comparison using a double-couple point source model for an earthquake,

$$\sigma_{\text{static}} = \frac{M}{4\pi r^3}, \tag{33}$$

where r is the distance from the volcano to the hypocenter and M is the seismic moment. Equation (33) is the stress in the direction of maximum amplitude and so is an upper bound on static stress change. Therefore the comparison with rectified diffusion presented in Figure 6 is conservative.

Figure 6 shows that in most triggering cases the pressure increase by rectified diffusion exceeds the static stress by factors of 100 or more. Certain eruptions seem more likely to have been triggered by such a mechanism than do others. For instance, the triggered phreatic activity at the mafic volcano Liamuiga is an excellent

Table 2. Documented Triggered Eruptions

Event Number	Volcano	Year	Distance, km	Delay, days	VEI	Earthquake Magnitude	SGVN
1	Robinson Crusoe[a]	1835	635	0	1?	8.5	1506-02=
2	Minchinmavida[a]	1835	664	0	2	8.5	1508-04=
3	Cerro Yanteles[a]	1835	733	0	2	8.5	1508-051
4	Peteroa[a]	1835	283	?	2	8.5	1507-04=
5	Liamuiga[b]	1843	116	0	?	8.2	1600-03=
6	Unnamed[b](15.97° N, 61.43° W)	1843	101	9	?	8.2	1600-07=
7	Llullaillaco[c]	1877	510	?	2	8.5	1505-11=
8	Ambrym[d]	1950	237	2	4	8.1	0507-04=
9	Karpinsky group[d]	1952	404	1	1	8.3	0900-35=
10	Tao-Rusyr Caldera[d]	1952	501	8	3	8.3	0900-31=
11	Puyahe	1960	226	2	3	9.5 M_w	1507-141

Earthquake magnitudes are M_s except where otherwise indicated and are estimated from intensities for preinstrumental events. The event numbers correspond to Figures 1 and 6. Distances are from epicenter to volcano. The delay is the time between the earthquake and the eruptive event. The volcanic explosivity index (VEI) and catalog number from the Smithsonian Global Volcanism Network (SGVN) are included for reference.

[a] *Darwin* [1896].

[b] *Robson and Towblin* [1966].

[c] *Casertano* [1963].

[d] *Newhall & Dzurisin* [1988].

Table 3. Calculated Values for Triggered Eruptions

Event Number	Volcano	$\delta_1 \times 10^5$	$\delta_2 \times 10^5$	Δt	Petrology	Model
1	Robinson Crusoe	1.2	0.42	55	basalt[a,b]	b
2	Minchinmavida	1.2	0.41	55	basalt[a,c]	b
3	Cerro Yanteles	1.2	0.37	55	basalt[a,d]	b
4	Peteroa	1.7	0.80	55	mafic andesite[a,e]	b
5	Liamuiga	2.6	1.6	49	basalt and andesite[f], phreatic	b
6	Unnamed	2.7	1.8	49	geyser ?	
7	Liullaillaco	1.3	0.50	55	dacite[g]	r
8	Ambrym	1.9	0.92	35	basalt[h]	b
9	Karpinsky group	1.5	0.60	44	andesite[i]	
10	Tao-Rusyr Caldera	1.4	0.5	44	andesite[j]	
11	Puyahe (Cordon Calle)	1.9	0.96	173	rhyolite/rhyodacite	r

The strains δ_1 and δ_2 are upper and lower limits on dynamic strain outside the magma body. Δt is the duration of the strong shaking in seconds. Petrology is the type of observed eruptive products. Model indicates the simplified system used for the case - either basalt (b) or rhyolite (r).

[a]The products were extrapolated from the general trends for the volcano.

[b]*Casertano* [1962].

[c]*Casertano* [1963].

[d]*Fuenzlida and Etchart* [1974].

[e]*Tormey et al.* [1989].

[f]*Robson and Towblin* [1966].

[g]*DeSilva and Francis* [1991].

[h]*McCall et al.* [1970].

[i]*Mooser et al.* [1958].

[j]*Newhall and Dzurisin* [1988].

candidate. The one case for which rectified diffusion is not significant in Figure 6 is the eruption of Puyahe triggered by the 1960 $M_w = 9.5$ Chile earthquake. In the case of this extremely large earthquake the volcano was effectively in the near field and it is likely that the direct deformation effects are important [*Barrientos*, 1994]. Note that these first-order calculations only account for the rectified diffusion caused by the largest amplitude wave. Smaller amplitude, longer duration waves may have significant effects as well.

8. Volcanic Tremor

Volcanic tremor may have an effect on magma chambers similar to that of distant regional earthquakes. Although the dynamic strains for tremor are much smaller than in tectonic events, the durations are longer. The dynamic strain can be estimated from the normalized displacements reported in the database of *McNutt and Garces* [1996]. Since the tremor source and the excited chamber are probably close to each other, we use an estimate of the dynamic strain 100 m from the source. Most of the examples in the database have a dynamic strain of the order of 10^{-11} - 10^{-7}. The higher end of the range is observed during eruptions.

Given that the dynamic strain of tremor is 2 - 6 orders of magnitude smaller than that reported in tectonic earthquakes, the duration of such events must be 4 - 12 orders of magnitude longer in order to have a comparable effect, i.e., Δt = 3.5 days - 10^6 yr. Rectified diffusion is not an important process for very small amplitude tremor. Larger amplitude tremor has been known to continue intermittently for days and in this context may be significant. When the above analysis is applicable, it would imply that rather than being only symptomatic, tremor can cause activity. Most proposed causes of tremor are based on the movement of either geothermal or magmatic fluids. One can therefore speculate that a positive feedback mechanism between seismicity and volcanism is in effect once tremor begins.

9. Conclusions

The above calculations indicate that rectified diffusion is a viable mechanism for explaining distant seismic triggering of volcanic eruptions. It must be remembered that these estimates of accumulated stress are based on simple, model systems. Effects such as rupture directivity and multicomponent volatile species have not been included. The inherent uncertainties in estimating physical parameters like bubble size and the dynamic strain amplitude prevent a more sophisticated treatment of such processes from being quantitatively useful. Furthermore, strong constraints have been placed on the magma-bubble system. Rectified diffusion is most effective in slightly supersaturated water-basalt systems with many small preexisting bubbles. The total porosity must be at least a few percent, and the radii of

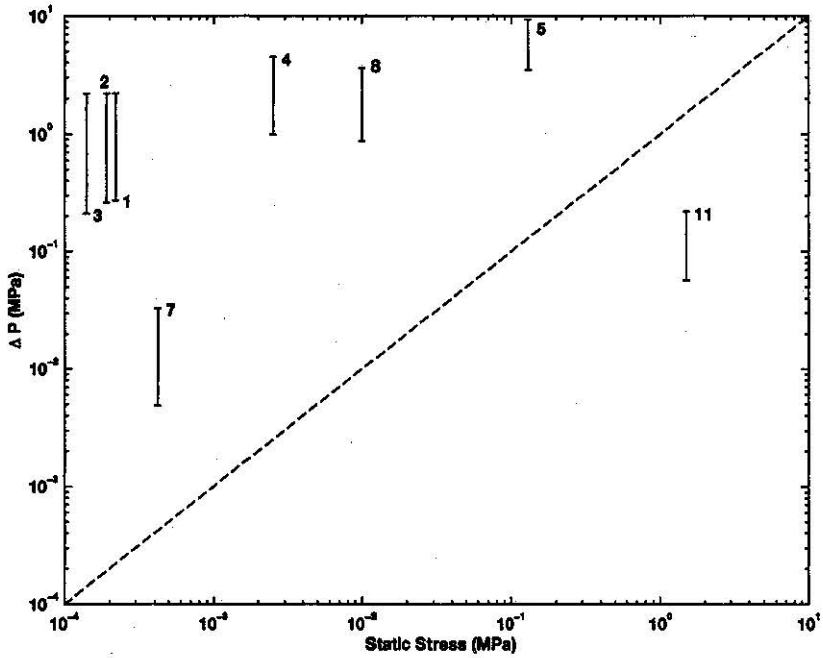

Figure 6. A comparison of the stresses from static strain and rectified diffusion for cases where a simple model system was applicable. Elastic stress change is calculated from equation (33) and plotted on the x axis. The minimum and maximum rectified diffusion pressures (ΔP) are calculated for each case at 1.3 x 10^2 MPa with a temperature of 1473 K for basalt and 1173 K for rhyolite. The results are plotted on the y axis. The range from maximum to minimum takes into account a range of δ corresponding to a range in possible hard-rock strains as estimated in equation (31) . Since the results are most sensitive to the estimates of δ and r_0, these are the largest sources of error in the calculations, and therefore the range shown can be taken as a crude estimate of the error bars. Results above the dashed line indicate that ΔP is larger than the static stress from the elastic model. Numbers correspond to the vent numbers in Table 2.

individual bubbles are assumed to be on the order of microns. The bubbles must have existed in a quasi-steady state until a regional earthquake disturbed the system. Despite these limitations, it is clear that rectified diffusion provides a more viable mechanism for explaining these events than has been provided to date. Future studies may demonstrate other mechanisms to be even more effective than rectified diffusion. However, it is important to realize that in a fluid system such as a magma chamber, a successful explanation of the observations requires incorporation of fluid dynamical mechanisms into seismological studies. This paper may be viewed as a case study of a particular mechanism that can provide a template for work to come.

Acknowledgments. Comments by M. Rutherford and J. Lowenstern greatly improved an early version of this manuscript. Reviews by T. Koyaguchi, S. Kaneshima, and an anonymous referee clarified several points. This paper is based on work supported under a National Science Foundation Graduate Fellowship and is contribution 5809 of the Division of Geological and Planetary Sciences, California Institute of Technology.

References

Barrientos, S.E., Large thrust earthquakes and volcanic-eruptions, *Pure Appl. Geophys., 142*, 225-237, 1994.

Blank, J.G., *An experimental investigation of the behavior of carbon dioxide in rhyolitic melt*, Ph.D. thesis, Calif. Institute of Technol., Pasadena, 1993.

Carragan, E., F. Michalko and S. Katz, Water wells in earthquake and explosion detection, *Rep. AFCRL-64-177*, Off. of Aerosp. Res., U.S. Air Force, Bedford, Mass., 1964.

Cashman, K. and M. Mangan, Physical aspects of magma degassing II: constraints on vesiculation processes from textural studies of eruptive products, in *Volatiles in Magma,Rev. Mineral.*, vol. 30, edited by M.R. Carroll and J.R. Holloway, pp. 447-478, Mineral Soc. of Am., Washington, D.C., 1994.

Casertano, L. *Catalogue of the Active Volcanoes of the World, Including Solfatara Fields: Part XV Chilean Continent*, 55 pp., International Volcanological Association, Napoli, Italy, 1962.

Casertano, L., General characteristics of active Andean volcanoes and a summary of their activities during recent centuries, *Bull. Seismol. Soc. Am., 53*, 1415-1433, 1963.

Crum, L.A., and G.M. Hansen, Generalized equations for rectified diffusion, *J. Acoust. Soc. Am., 72*, 1586-1592, 1982.

Darwin, C., *Journal of Researches Into the Natural History and Geology of Countries Visited During the Voyage of H.M.S. Beagle Round the World*, Appleton, New York, 1896.

Davis, M. J., and P. D. Ihinger, Crystal nucleation on bubbles in hydrous silicate melt, *Eos Trans. AGU, 77*, (46), Fall Meet. Suppl., F819, 1996.

DeSilva, S.L., and P.W. Francis, *Volcanoes of the Central Andes*, Springer-Verlag, New York, 1991.

Dixon, J.E., *Water and carbon dioxide in basaltic magmas*, Ph.D. thesis, Calif. Inst. of Technol.,Pasadena,, 1992.

Dixon, J.E., An experimental study of water and carbon dioxide solubility in mid-ocean ridge basaltic liquids, Part I: Calibration and solubility models, *J. Petrol., 36*, 1607-1631, 1995.

Eller, A., Growth of bubbles by rectified diffusion, *Jour. Acoust. Soc. Am., 46*, 1246-1250, 1969.

Eller, A. and H.G. Flynn Rectified diffusion during nonlinear pulsations of cavitation bubbles, *J. Acoust. Soc. Am., 37*, 493-503, 1965.

Fuenzalida, P.R. and H. Etchart, Evidencias De Migracion Volcanica Recient Desde La Linea De Volcanes De La Patagonia Chilena, *Proc. Sympos. "Andean and Antarctic Volcanology Problems"*, 392, 1974.

Holloway, J.R., Fugacity and activity of molecular species in supercritical fluids, in *Thermodynamics in Geology*, edited by D.G. Fraser, pp. 161-180, D. Reidel, Norwell, Mass., 1977.

Houston, H., and H. Kanamori, Comparison of strong-motion spectra with teleseismic spectra for three magnitude 8 subduction-zone earthquakes, *Bull. Seismol. Soc. Am., 80*, 913-934, 1990.

Hsieh, D.-Y., and M. S. Plesset, Theory of rectified diffusion of mass into gas bubbles, *J. Acoust. Soc. Am., 33*, 206-215, 1961.

Hurwitz, S., and O. Navon, Bubble nucleation in rhyolitic melts: Experiments at high pressure, temperature, and water contents, *Earth Planet. Sci. Lett., 122*, 267-280, 1994.

Johnson, M.C., A.T. Anderson, and M.J. Rutherford, Pre-eruptive volatile contents of magmas, in *Volatiles in Magmas Rev. Mineral.*, vol. 30, edited by M.R. Carroll and J.R. Holloway, pp. 281-330, Mineral. Soc. of Am., Washington, D.C.,1994.

Kieffer, S.W., Sound speed of liquid-gas mixtures: Water-air and water-steam, *J. Geophys. Res., 82*, 2895-2904, 1977.

Kimura, M., Significant eruptive activities related to large interplate earthquakes in the Northwestern Pacific margin, in *Geodynamics of the Western Pacific*, edited by S. Uyeda, R.W. Murphy and K. Kobayashi, pp. 557-570, Jpn. Sci. Soc., Tokyo, 1978.

Lambert, G., M.F. Cloarec, B. Ardouin, and J.C. LeRoully, Volcanic emission of radionuclides and magma dynamics, *Earth Planet. Sci. Lett., 76*, 185-192, 1985.

Leighton, T.G., *The Acoustic Bubble*, Academic, San Diego, Calif., 1994.

Lowenstern, J. B., Applications of silicate-melt inclusions to the study of magmatic volatiles, in *Magmas, Fluids, and Ore Deposits*, edited by J.F.H. Thompson, pp. 71-100, Miner. Assoc. of Can., 1995.

McCall, G.J.H., R.W. LeMaitre, A. Malahoff, G.P. Robinson, and T.J. Stephenson, The geology and geophysics of the Ambrym Caldera, New Hebrides, *Bull. Volcanol., 34*, 681-696, 1970.

McNutt, S.R., and M.A. Garces, Constraints on volcanic tremor source models from worldwide measurements of tremor amplitudes, frequencies, wave types and durations, *NSF Final Proj. Rep. 9418219*, Natl. Sci. Found., Washington, D.C., 1996. (Tremor database available at http://www.giseis.alaska.edu/dbases/dbaselead.html.)

McTigue, D.F., Elastic stress and deformation near a finite spherical magma body: Resolution of the point source paradox, *J. Geophys. Res., 92*, 12,931-12,940, 1987.

Mooser, F., H. Meyer-Abich, and A.R. McBirney, *Catalogue of the Active Volcanoes of the World, Including Solfatara Fields: Part V Melanesia*, 146 pp., International Volcanological Association, Napoli, Italy, 1958.

Murase, T., and A.R. McBirney, Properties of some common igneous rocks and their melts at high temperatures, *Geol. Soc. Am. Bull., 84*, 3563-3592, 1973.

Newhall, C.G., and D. Dzurisin, Historical unrest at large calderas of the world, *U.S. Geol. Surv. Bull., 1855*, 1988.

Pan, V., J.R. Holloway, and R.L. Hervig, The pressure and temperature dependence of carbon dioxide solubility in tholeiitic basalt melts, *Geochim. Cosmochim. Acta, 55*, 1587-1595, 1991.

Robson, G.R., and J.F. Towblin, *Catalogue of the Active Volcanoes of the World, Including Solfatara Fields: Part XX West Indies*, 55 pp., International Volcanological Association, Napoli, Italy, 1966.

Shaw, H.R., Comments on viscosity, crystal settling, and convection in granitic magmas, *Am. J. Sci., 263*, 120-152, 1965.

Silver, L.A., P.D. Ihinger, and E. Stolper, The influence of bulk composition on the speciation of water in silicate glasses, *Contrib. Mineral. Petrol., 104*, 142-162, 1990.

Simkin, T., and L. Siebert, *Volcanoes of the World: A Regional Directory, Gazetteer and Chronology of Volcanism During the Last 10,000 Years*, Geoscience, Tucson, Ariz., 1994.

Strasberg, M., Rectified diffusion: comments on a paper of Hsieh and Plesset, *J. Acoust. Soc. Am., 33*, 259, 1961.

Sturtevant, B., H. Kanamori, and E. E. Brodsky, Seismic triggering by rectified diffusion in geothermal systems, *J. Geophys. Res., 101*, 25,261-25,282, 1996.

Tormey, D.R., F.A. Frey, and F.L. Escobar, Geologic history of the Active Azufre-Planchon-Peteroa Volcanic Center (35°15'S, Southern Andes), with implications for the development of compositional gaps, *Assoc. Geol. Argent. Rev., 44*, 420-430, 1989.

Watson, E.N., Diffusion in volatile-bearing magmas, in *Volatiles in Magma,Rev. Mineral.*, vol. 30, edited by M.R. Carroll and J.R. Holloway, pp. 371-411, Mineral Soc. of Am., Washington, D.C., 1994.

Yamashina, K., and K. Nakamura, Correlations between tectonic earthquakes and volcanic activity of Izu-Oshima Volcano, Japan, *J. Volcanol. Geotherm. Res., 4*, 233-250, 1978.

Zhang, Y., and E.M. Stolper, Water diffusion in a basaltic melt, *Nature, 351*, 306-309, 1991.

Zhang, Y., E.M. Stolper, and G.J. Wasserburg, Diffusion of water in rhyolitic glasses, *Geochim. Cosmochim. Acta, 55*, 441-456, 1991.

E. E. Brodsky and H. Kanamori, Seismological Laboratory, MC 252-21, California Institute of Technology, Pasadena, CA 91125. (email: brodsky@gps.caltech.edu; hiroo@gps.caltech.edu)

B. Sturtevant, Graduate Aeronautics Laboratories, California Institute of Technology, Pasadena, CA 91125. (email: brad@galcit.caltech.edu)

(Received October 10, 1997; revised June 9, 1998; accepted June 17, 1998.)